^{13}C labeling of the tricarboxylic acid cycle and carbon conversion efficiency in lesquerella (*Physaria fendleri*) embryos.

Undergraduate Research Thesis

Presented in partial fulfillment of the requirements for graduation *with honors research distinction* in Biochemistry in the undergraduate colleges of The Ohio State University

by

Brooke Anderson

The Ohio State University
May 2015

Project Advisor: Ana Paula Alonso, Department of Molecular Genetics

Abstract

Lesquerella (Physaria fendleri) is a Brassicaceae that produces a valuable class of compounds in its embryos called hydroxy fatty acids. These fatty acids are used widely in industry to produce cosmetics, coatings, greases, plastics, paints, and biofuel, among others. The current source of hydroxy fatty acids is ricinoleic acid from the castor plant (Ricinus communis), which also produces the highly toxic compound ricin that has eliminated castor plant cultivation in the United States. Lesquerella produces lesquerolic acid, a hydroxy fatty acid with only two additional carbons as compared to ricinoleic acid, which therefore performs in a chemically similar manner. Since it is non-toxic and already grows in the wild in the southwest US as a winter annual that will not compete with food crops, lesquerella could serve as a suitable alternative to castor oil. However to become economically viable, lesquerella first must be engineered to produce more of these fatty acids to meet demands.

Background

Lesquerella (*Physaria fendleri*) is being considered as a domestic crop to produce hydroxy fatty acids (HFAs) for a large variety of industrial purposes: in manufacturing they are used in lubricants and greases; in production they are added to cosmetics, paints, plastics, coatings, and more; and in the biofuel industry they can be modified to form superior estolides, which are oligomeric esters formed from the condensation two fatty acids (hydroxyl group of a HFA and carboxyl end of a second fatty acid); these can be added to diesel fuel as a lubricant (Goodrum et al., 2004). HFAs are highly valued for their viscosity and lubricant properties in cold-temperature ranges and for their limited solubility in aliphatic solvents (Cermak et al., 2006, Kim et al., 2013). It has been suggested that HFA-based products are superior to petroleum-based ones and that these oils can relieve some dependence on fossil fuels used in industry (Kim et al., 2013).

The current source of hydroxy fatty acids for industry is castor oil, an import worth up to 110 million dollars in 2011 (obtained from USDA Foreign Agricultural Service's Global Agricultural Trade System, http://apps.fas.usda.gov/gats/). Although *Ricinus communis*, the castor plant, grows best in tropical regions, it has been known to grow as a weed in the southern United States. However, the castor bean contains ricin, a highly toxic compound that has led the US to ban commercial growth of the plant. Therefore, the US imports all of its castor oil, with the vast majority coming from India. The HFA of value in castor is ricinoleic acid (12-OH $18{:}1\Delta^{9}$). Lesquerolic acid, the HFA synthesized and stored in lesquerella embryos, has only two more carbons before the double bond than ricinoleic acid and therefore it has all the same valuable chemical properties as castor oil (Figure 1). While the biosynthetic pathway of lesquerolic acid has not been elucidated, studies in *Arabidopsis thaliana* containing the castor

hydroxylase gene have suggested that either the hydroxylating enzyme can accept both oleic acid ($C18:1\Delta^{9}$) and eicosenoic acid ($C20:1\Delta^{11}$) or that lesquerolic acid is a product of an elongase acting on ricinoleic acid (Broun and Somerville, 1997). Since *P. fendleri* accumulates no ricinoleic acid, it is estimated that in the case of this second hypothesis, that the elongating enzyme is extremely efficient (Moon et al., 2001).

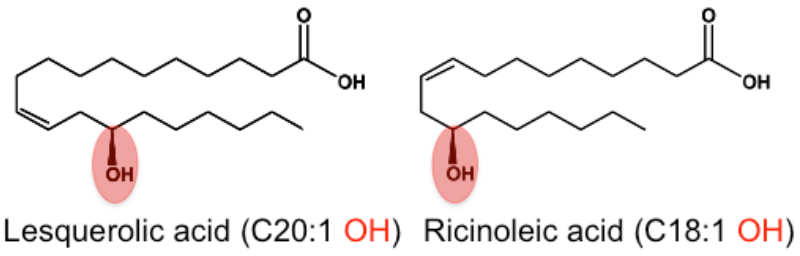

Figure 1. Lesquerolic acid from *Physaria fendleri* (lesquerella) versus ricinoleic acid from *Ricinus communis* (castor).

As an alternative crop, lesquerella is ideal. It is non-toxic and already grows natively in the southwest U.S. as a winter annual without interfering with commercial food crops. Once oils have been pressed out of the seeds, the remaining seed meal harbors at least two more commercial resources: first, a unique polysaccharide gum that can be used as an industrial thickener (Abbott et al. 1994); and second, a significant amount of protein—30% of the defatted meal—whose amino acid composition (similar to soybean and high in lysine, methionine, and threonine) should be suited for use as a protein supplement for animal fodder (Carlson et al., 1990). The lesquerella plant naturally contains 25% oil (w/w) of which 60% is lesquerolic acid (Barclay et al., 1962); however, this is not enough lesquerolic acid for lesquerella to be commercialized as an economically viable alternative. It is therefore critical to improve the oil content of lesquerella to have an increased lesquerolic acid content. The lesquerella plant is a member of the Brassicaceae family and a winter annual that grows well with limited fertilizer and water application, making it a desirable crop in arid regions. Field trials have determined that lesquerella yield is greatest when planted at a rate of 8-12 kg/ha (Brahim et al., 1996) in October

using the same tools as for alfalfa. There is very small growth through January, and then the vegetative canopy grows rapidly through March. Flowering and seed development lasts through May and seeds are collected via combine by late June, again using the same tools as used for alfalfa. Irrigation is most important before emergence and between February and May, during which time 90% of the growth of lesquerella takes place. Current seed yields are around 2000 kg/ha, but through breeding and improving agronomic practices the plant has the potential to reach 2500-3000 kg/ha (Dierig, 2011).

Genetic engineering for improvement is also possible since lesquerella is a Brassicaceae and can therefore be modeled by the fully sequenced *Arabidopsis thaliana* genome. To this end, two successful methods for transforming lesquerella have been identified: *Agrobacterium tumefaciens*-mediated transformation of calli (Wang et al., 2008) and biolistic leaf plastid transformation (Skarzhinskaia et al., 2002).

To increase the oil yield of lesquerella, we have been working towards identifying targets for engineering the plant through a metabolomic and fluxomic approach. For this engineering to be done, it is first necessary to map out the metabolic pathways involved in oil synthesis in order to identify targets that can be altered for the most efficient increase in fatty acid production. In plants, the synthesis of fatty acids (Figure 2) requires carbon in the form of acetyl-coenzyme A (acetyl-CoA), energy (ATP), and reductant (NAD(P)H).

To this end, the growth of key biomass components (starch, protein, and fatty acids) has been charted and intracellular metabolites involved in biochemical pathways in lesquerella have been quantified (i.e., metabolomics). The biomass results showed that the main catabolic product at early lesquerella embryo development was protein (ratio of fatty acids:protein = 0.7) at the torpedo stage but that this main anabolism product switched over to fatty acids (fatty acids:

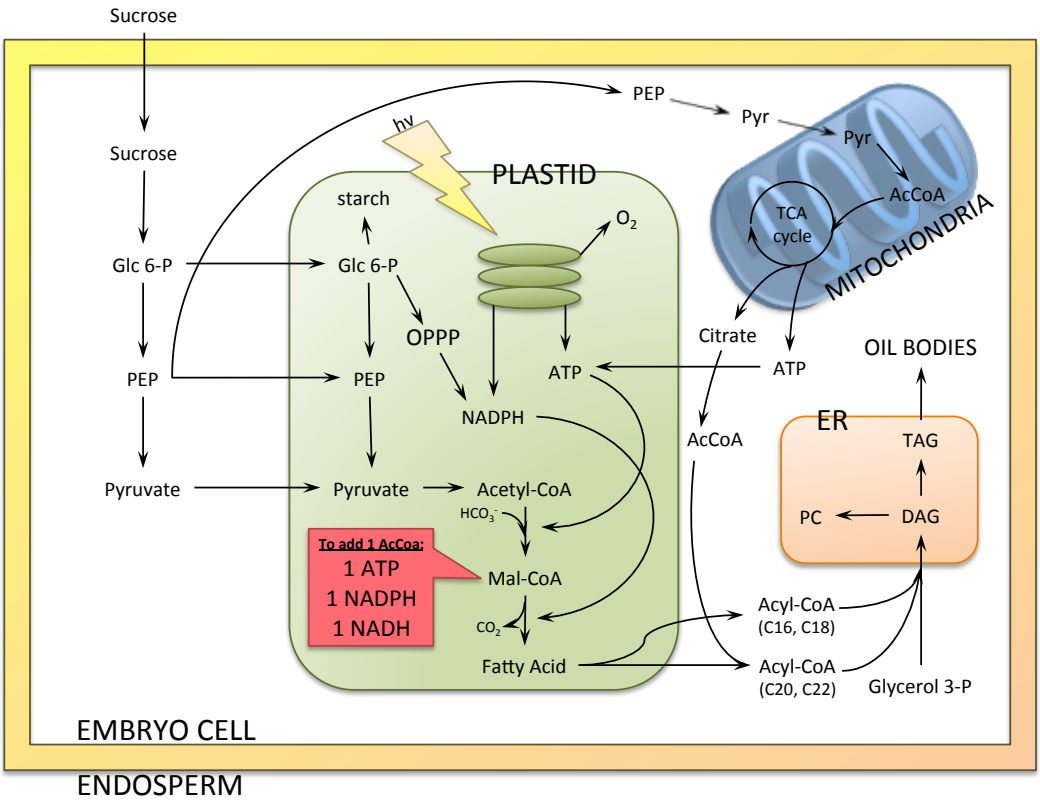

Figure 2. Fatty acid synthesis in photosynthetic seeds. Acetyl-CoA generated from pyruvate is used as the 2-carbon building block for fatty acid synthesis. Acetyl-CoA carboxylase is used to create Mal-CoA from acetyl-coA and from this fatty acid synthase is used to elongate the fatty acid. Each additional AcCoa addition requires the inputs shown in the red box. Fatty acids are exported to the cytosol and converted to acyl-CoA for active incorporation onto a G 3-P glycerol backbone at the ER to form membrane phospholipids (PC) and storage oils (TAG). [Glc 6-P, glucose 6-phosphate; PEP, phosphoenolpyruvate; OPPP, oxidative pentose phosphate pathway; Mal-CoA, malonyl-Coenzyme A; AcCoa, acetyl-Coenzyme A; Pyr, pyruvate; G 3-P, glycerol 3-P, glycerol 3-phosphate; DAG, diacylglycerol; TAG, triacylglycerol; PC, phosphatadylcholine (phospholipids)

protein = 2.1) for mature embryos. The targeted metabolomics experiment showed that malate and citrate are the main organic acids in lesquerella embryos, indicating that they might be the main carbon precursors for fatty acids (Cocuron et al., 2014). The metabolomics study also revealed the occurrence of key pathways involved in fatty acid synthesis: (i) the oxidative portion of the pentose phosphate pathway that generates NADPH; (ii) the tricarboxylic acid cycle which produces both NADH and ATP by oxidative phosphorylation; and (iii) photosynthesis that generates NADPH and ATP. However, the relative contribution of each of these pathways to the synthesis of fatty acids (in terms of carbon, energy, and reductant) can only be determined by measuring the metabolic flux throughout each.

Therefore the next step in identifying targets for increasing fatty acid production—mapping out the rates of carbon transfer throughout the pathways of creating fatty acids to find

where the rate of transfer is limiting synthesis—uses a method called ^{13}C-based metabolic flux analysis. In brief, the experiment will aim to deliver carbon-13 to lesquerella embryos in culture plates, in an imitation of the way lesquerella embryos take up carbon and nitrogen sources from the endosperm *in planta*.

To mimic the growth of embryos within the plant while growing embryos in culture plates, a culturing medium was modeled based on the endosperm composition in lesquerella seeds. The two main carbon sources were found to be glucose and sucrose and the main nitrogen source to be glutamine (Alonso lab unpublished data); therefore these three compounds were used as carbon and nitrogen sources for the *in vivo* culturing medium.

Analyzing the ^{13}C-labeling of intracellular metabolites in cultured embryos will create a carbon flux map of primary metabolism to chart the catabolism and anabolism of compounds used in fatty acid synthesis, acetyl-CoA, NADPH, and ATP. This map is predicted to identify one or more bottlenecks in production of these fatty acid components and these bottlenecks can be targeted for engineering a high-oil lesquerella. Results at present include the mass isotopomer abundances in labeled lesquerella embryos of six organic acids of the tricarboxylic acid (TCA) cycle. This metabolic cycle plays an important role in examining the carbon base for fatty acids, acetyl-CoA. The pools of this compound comes from sugars, which pass through glycolysis, from citrate in the TCA cycle through citrate lyase, and from malate transported into chloroplasts and cleaved by plastidic malic enzyme (Figure 2). Also contributing to the labeling patterns in the cycle is glutamine, which shows up as a side pathway that contributes to alpha-ketoglutarate (AKG).

Materials and methods

Chemicals: All unlabeled standards, 3 N methanolic/HCl, and toluene were obtained from Sigma-Aldrich (St. Louis, MO). ^{13}C-labeled glucose, sucrose, and glutamine were all ordered from Isotec (Miamisburg, OH). Solvents for GC-MS and LC-MS/MS were purchased from Fisher Scientific (Pittsburgh, PA).

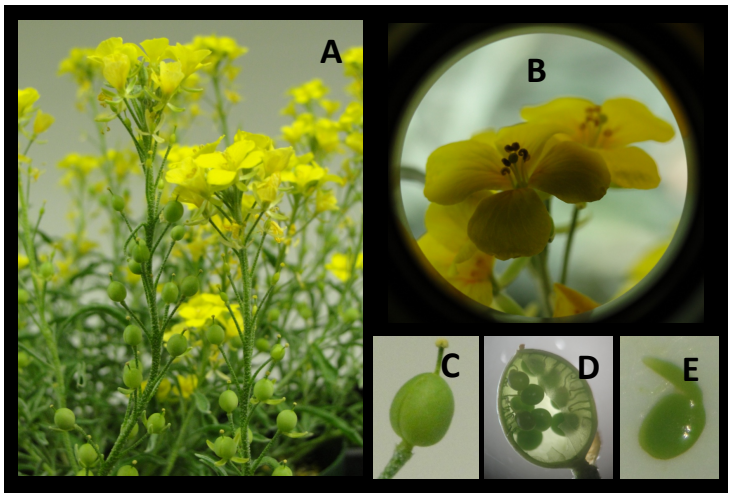

Figure 3. Production of embryos by *Physaria fendleri* syn. Lesquerella (Cocuron et al. 2014). (A) Lesquerella plants grown in controlled-environment chambers. (B) Flowers were cross-pollinated upon blooming and tagged to mark the start of embryo development. (C) Growing seed pod. (D) Inside of seed pod, containing developing seeds. (E) Developing embryo, dissected from seeds under a microscope.

Plant growth: *Physaria fendleri* plants were grown in 18-cm pots in a 22 °C growth chamber under light of 320 µmol per m^2 per second during a 16-h/8-h day/night photoperiod. The seeds were planted in autoclaved soil supplemented with 6 g of time-release fertilizer. When initial bud development was observed, plants were thinned to one per pot and plants were treated with 5 g of additional fertilizer. Flowers were hand pollinated and marked at pollination to track embryo development as days after pollination (DAP) (Figure 3).

Embryo collection: For control embryos *in planta* biomass analysis, siliques were collected at 27 days after pollination (DAP) and embryos were dissected under a microscope and kept on ice while collecting batches of 15 embryos in 2 mL tubes (Figure 4). The embryos were freeze-dried by lyophilizing and stored at -80°C until analyzed as a control for cultured embryos.

Figure 4. *In planta* embryo development (Cocuron et al. 2014). Embryos were collected at 18 DAP for culturing and 27 DAP for *in planta* controls for the cultured embryo analyses.

For culturing embryos, siliques were collected at 18 and 19 DAP. All analyses following collection took place under sterile conditions at a clean bench. Siliques were washed with bleach for 5 min then rinsed four times with autoclaved ddH2O. Embryos were extracted under a dissecting microscope and placed in prepared culture plates, 10 embryos per well.

Embryo culturing: The medium buffer preparation consisted of glucose, sucrose, glutamine, HEPES buffer, Murashige & Skoog salt, and Gamborg vitamin mixture, with a final pH of 6.3. This preparation was filtered under sterile conditions using a syringe equipped with a 0.22 micron filter and then stored for use at 4 °C for up to two weeks. This final medium for culturing, prepared under sterile conditions, consisted of medium buffer, polyethyleneglycol, and abscissic acid.

Three different labeled culturing mediums were prepared in addition to the unlabeled medium described previously. The three experiments replaced either glutamine or glucose with labeled versions of these compounds in the same total concentration: (1) Labeled ^{13}C glucose: 20% [U-^{13}C6] glucose and 80% [1,2-^{13}C2] glucose; (2) Labeled ^{13}C-glutamine: [U-^{13}C5] glutamine; (3) 20% ^{13}C-labeled: 20% [U-^{13}C5] glutamine, 20% [U-^{13}C6] glucose, and 20% [U-^{13}C12] sucrose.

The whole culturing procedure was performed at a clean bench under sterile conditions. Culturing wells were equipped with double glass filters to prevent anoxia during incubation and then 1 mL of final prepared medium was added. Embryos were dissected as described before. Five mL of sterile water was added in open areas between circular wells, and 1.5 mL of water was added to any well without embryos. The plate lid was closed with Millipore tape and placed in a shallow well of water for incubation. Growing embryos were incubated for 9 days at 21 °C under 24 hours constant light to establish a steady rate of media consumption and metabolic

processing. A beaker of water was left in the incubating chamber to maintain humidity.

Embryos were removed from the incubator after 9 days. These embryos were collected in a sieve and washed with distilled water, surface dried with kimwipes, then freeze dried in a pre-weighed 2 mL tube by a lyophilizer for three days. The dried embryos were weighed in their tube to determine their dry weight.

Media analysis for rates of substrate uptake and carbon conversion efficiency (CCE): To account for any evaporation during the incubation period, additional wells were prepared exactly the same with water in unused wells and the proper amount of medium and filters in control wells but no embryos. At the end of incubation and embryo collections, all remaining media and the filters were collected in separate tubes and each well was washed with 4 x 1 mL water. The tubes were vortexed thoroughly and 1 mL was sampled and centrifuged. Twenty-five μL of this was mixed with an internal standard of 4 mM [U-^{13}C]-glucose and 2 mM [U-^{13}C]-glycine and diluted for LC-MS/MS analysis.

Biomass characterization of cultured embryos:

Sequential extractions: Fatty acids were extracted from embryos with non-polar solvents. To the embryos, 950 μL 2:1 hexane:isopropanol and 50 μL of 1 mg/mL triheptadecanoin (internal standard) were added along with a 5 mm tungsten bead and the mixture was ground and homogenized in a mill mixer at 30 Hz for 5 minutes. The tubes were centrifuged at 13,000 x g for 10 minutes and the supernatant was retained in glass tubes. These steps were repeated two more times, without adding the internal standard, with 1 mL then 0.5 mL of 2:1 hexane:isopropanol. The embryo pellets that remained after this oil extraction were dried under

nitrogen and stored at -80 °C for protein extraction. The lipid extractions were dried down under nitrogen for methylation, to cleave triacylglycerol (TAG) fatty acids from their glycerol backbones and to create volatile fatty acid methyl esters (FAMEs). To solubilize the dried lipid extracts, 0.5 mL 3N methanol/HCl and 150 µL toluene were added and the mixtures were homogenized by vortexing. Oxygen was purged from the tubes with nitrogen gas. Then the tubes were incubated at 80 °C to react for two hours, vortexing to re-homogenize every half hour. After briefly cooling, the reaction was quenched using 250 µL 5% (w/v) $NaHSO_4$. To this, 1 mL hexane was added in and vortexed, then the tubes were centrifuged at 2000 rpm (560 x g) for 10 minutes to separate the polar and non-polar layers. The upper non-polar layer containing FAMEs was drawn off and 200 µL of this layer was diluted with 800 µL hexane for GC-MS analysis.

Protein extractions were completed on the pellet remaining after extracting fatty acids. To the dried pellet was added 0.5 mL of protein extraction buffer (20 mM Tris-HCl, pH 7.5, 150 mM NaCl, and 1% (w/v) SDS), preheated to 42 °C. These tubes were vortexed for 15 minutes at 42 °C, then centrifuged at 13,000 x g for 10 minutes, and then the supernatant containing extracted proteins was collected in a 1.5 mL tube. A second 0.5 mL of warmed buffer was added to the remaining pellet, vortexed for 10 minutes at 42 °C, centrifuged as before, and then the supernatant from this second extraction was combined with the supernatant collected before.

Starch extractions were performed on the pellet remaining after extracting proteins. Pellets were resuspended with 1 mL of water and centrifuged at 13,000 x g, then supernatant was discarded. The pellet was washed once more with 1 mL water. Then 250 µL of 0.1 M acetate buffer, pH 4.8 was added to the pellets and tubes were autoclaved for 1 hour at 120 °C and 21 psi. After briefly cooling, 490 µL more of the acetate buffer and 33 units of amyloglucosidase (Megazyme International Ireland LTD Total Starch Assay Kit) was added to each tube. The

tubes were incubated at 55 °C for 1 hour and then centrifuged at 13,000 x g for 15 minutes. Five hundred μL of the supernatant containing starch extract was collected for LC-MS/MS quantification.

Quantification: Fatty acid content was determined by gas chromatography-mass spectrometry. The fatty acid methyl ester derivatives were analyzed using a Thermo Trace gas chromatograph ultra, coupled to a single quadrupole DSQ II mass spectrometer, using the same equipment and settings as detailed by Tsogtbaatar et al., 2015 with the one modification that the last ramp lasted 5 min longer. GC-MS data was analyzed using Xcalibur software and FAME derivatives were identified using a combination of FAME standards from Sigma and the NIST library.

Protein content was quantified using Bio-Rad's DC Protein Assay kit, which uses a modified Lowry method for colorimetric protein quantification. A BSA standard curve was generated alongside samples using the kit.

Starch glucosyl units from amyloglucosidase activity were quantified using LC-MS/MS. Five μL of extract was diluted 200x with (60:40) acetonitrile:water and 10 μL of diluted sample for LC-MS/MS analysis. The LC-MS/MS acquisition method used was as according to the sugar- and sugar alcohol-detecting method detailed in Cocuron et al., 2014.

TCA labeling: Water-soluble intracellular metabolites were extracted from embryos using a boiling water method. Freeze-dried embryos collected from culturing were ground in a mixer mill with a 5 mm tungsten bead for 2 min at 30 Hz. To each tube of pulverized embryos was added 1 mL of boiling ddH_2O, then the tube was immediately placed in a 100 °C water bath. Each tube was boiled for 10 minutes, vortexing to resuspend halfway through. These tubes were

placed on ice to cool then centrifuged at 13,000 x g, temperature 4 °C, for 5 minutes. The supernatant was pipetted into a syringe equipped with a 0.22 µm filter, and filtered supernatant was collected in a falcon tube. The remaining embryo pellet was washed with 1 mL ddH_2O, vortexed, and centrifuged as before. This supernatant was also pipetted into the filter-syringe using the same pipette tips, and filtered supernatant combined with the first fraction. The syringe and filter was lastly rinsed with 2 x 1 mL ddH_2O, the rinse water collected with the supernatants. Falcon tubes were centrifuged in a benchtop centrifuge to collect all extract in one volume, and then the tubes were frozen in liquid nitrogen and freeze-dried in a lyophilizer for 24 hours.

Metabolite extract was separated and purified using stacked ion exchange columns (Figure 5). Both columns were built using 5¾" pasteur pipettes then adding sequentially a small amount of glass wool, 140 µL white quartz 70 mesh sand treated with HCl, 1 cm resin, then 140 µL more sand. The cation exchange resin was Dowex 50x4-200. The prepared column was rinsed with first 5x1 mL ddH_2O, then 5x1 mL 1 N NH_4OH, ddH_2O again, 5x1 mL 1 N HCl, then ddH_2O to keep from drying out. The anion exchange resin was Dowex 1x8-200 mesh. The prepared column was rinsed with first 5x1 mL ddH_2O, then 5x1 mL 4 M formic acid, then ddH_2O to keep from drying out.

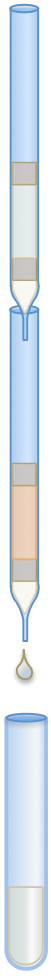

Figure 5. Stacked purification columns. A cation exchange column, capturing amino acids, was stacked on top of an anion exchange column, trapping organic acids and phosphorylated compounds.

Lyophilized metabolite extraction samples were resuspended in 300 µL of ddH_2O then transferred to NANOSEP® 0.2 µm microfilter tubes to centrifuge and filter samples at 13,000 x g at 4 °C for 45 minutes. Lastly 1 mL 0.01 N HCl was added to each sample tube. One hundred µL of this unpurified sample was retained for evaluating the efficiency of the purification

technique and for analyzing phosphorylated compounds, which are degraded by the 4 M formic acid used to elute compounds out of the anionic exchange column.

To run the samples, the cation exchange column was stacked on top of the anion exchange column, and the water was drained from the two columns. A glass tube was placed under the columns and the sample applied to the top column. The sample tube was rinsed with 1 mL 0.01 M HCl, and this was also applied to the column. Once the sample migrated through both columns, 5 x 1 mL ddH_2O was used to wash the columns. This first saved fraction, comprising of the run through and washes, contained sugars and sugar alcohols. Then, the two columns were separated to elute their compounds into separate glass tubes. The cation exchange column was washed with 1 M NH_4OH to elute amino acids and the anion exchange column was washed with 4 M formic acid to elute organic acids and phosphorylated compounds. All fractions were dried under nitrogen gas at 50 °C for 45 minutes. Tubes were frozen by pouring liquid nitrogen over them and then the tubes were lyophilized for 24 hours.

To analyze the organic acid intermediates of the TCA cycle, samples were separated by liquid anion exchange chromatography using an IonPac AS11 guard column (250 x 2 mm, Dionex) and detected by a triple quadrupole AB Sciex 5500 mass spectrometer (MS) in negative ionization mode. The collision cell parameters of the MS were set to detect organic acid fragments that had lost water (malate, succinate, citrate, isocitrate) or CO_2 (fumarate and AKG), allowing the observation of a parent/daughter ion pair for each organic acid (Supplementary 1). Multiple reaction monitoring (MRM) mode allowed the detection of all the parent/daughter ion pairs for each mass isotopomer simultaneously. The method used for LC-MS/MS data acquisition was as previously described (Koubaa et al., 2013).

Results

Culturing conditions: To grow embryos with labeled-substrates, a culture medium had to be created so that cultured-embryo growth would mimic that of embryos *in planta*. A series of embryo cultures were completed with varying quantities of the *in planta* carbon and nitrogen sources (glucose, sucrose, and glutamine), hormones (PEG and ABA) and light level to accumulate the same amount of dry weight, and same percentage of the key biomass components: fatty acids, proteins, starches, and cell wall. Embryos were dissected out of seeds at 18 DAP and only embryos whose hypocotyls were bent between 30 and 90 degrees with respect to the cotyledons were selected for culturing, 8 per each well. After growing for 9 days at 21 °C under continuous light, cotyledons had enlarged considerably and separated from each other since they were not constricted by a seed coat as those of the *in planta* were (Figure 6).

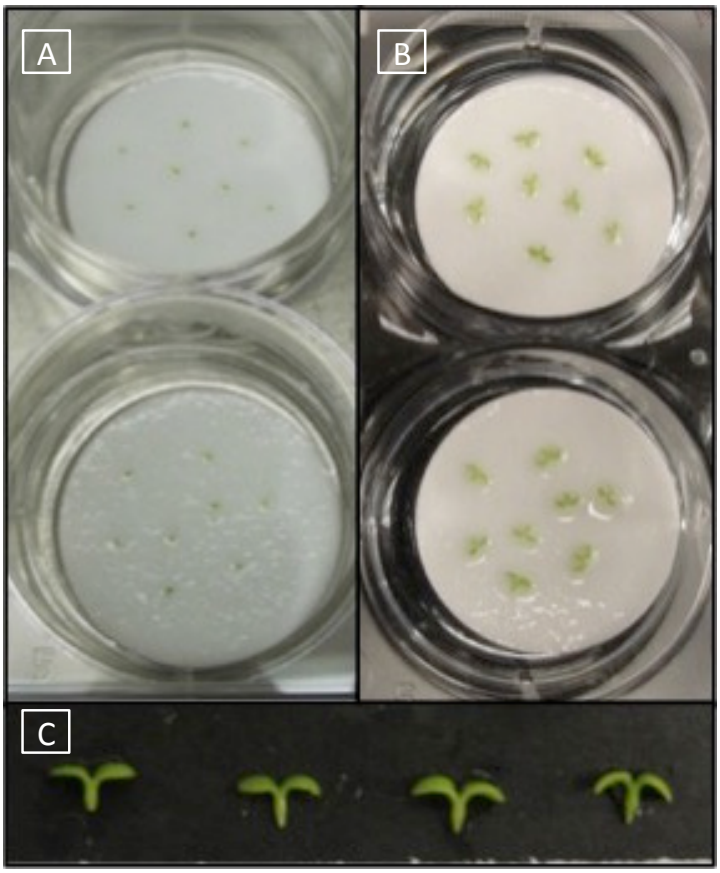

Figure 6. Cultured embryos in petri dish wells containing two filters and 1 mL prepared growth medium at (A) before incubating, at 18 DAP and (B) after growing for 9 days at 21 °C under constant light. (C) A representative embryo from each well (biological replicate) of one culture plate.

As different culture media were attempted to determine culture conditions, cultured embryos were put through sequential biomass extractions alongside *in planta* controls. The *in*

Table 1. (A) Dry weight and biomass composition and (B) fatty acid profile of in planta versus cultured *P. fendleri* embryos. Standard deviations are produced from 3 biological replicates, and components that are significantly different are marked with an asterix.

(A)	dry weight (mg/emb)		TAG content (%)		Protein content (%)	
	AVG	ST. DEV.	AVG	ST. DEV.	AVG	ST. DEV.
In planta	0.16	+/- 0.01	27.2%	+/- 4.1%	35.4%	+/- 4.0%
Cultured	0.14	+/- 0.01	25.7%	+/- 0.9%	32.0%	+/- 1.7%
p-value	0.08		0.96		0.28	
	Starch content (%)		Cell wall (%)			
	AVG	ST. DEV.	AVG	ST. DEV.		
In planta	5.0%	+/- 2.4%	32.4%	+/- 10.5%		
Cultured	4.0%	+/- 0.2%	38.3%	+/- 2.8%		
p-value	0.74		0.24			

(B)	C16:0		C18:0		*C18:1		C18:2	
	AVG	ST. DEV.	AVG	ST. DEV.	AVG	ST. DEV.	AVG	ST. DEV.
In planta	2.8%	+/- 0.3%	2.1%	+/- 0.1%	17.3%	+/- 0.3%	10.5%	+/- 0.4%
Cultured	4.2%	+/- 1.1%	3.1%	+/- 0.7%	24.9%	+/- 0.4%	12.2%	+/- 1.3%
p-value	0.14		0.14		<0.01		0.14	
	C18:3		*C20:1-OH		C20:2-OH			
	AVG	ST. DEV.	AVG	ST. DEV.	AVG	ST. DEV.		
In planta	13.2%	+/- 0.8%	49.7%	+/- 0.3%	4.5%	+/- 1.0%		
Cultured	14.8%	+/- 0.9%	35.3%	+/- 1.4%	5.5%	+/- 1.3%		
p-value	0.14		<0.01		0.40			

planta controls' biomasses and fatty acid profiles matched the values published by Cocuron et al., 2014, indicating the success of experimental methods. Cultured embryos from the finally-tested medium were shown to have the same biomass percentage of fatty acids, proteins, and starches within standard deviations (Table 1A). While the percentage of total fatty acids were equal in cultured and *in planta* embryos, the specific fatty acid profiles showed some differences (Table 1B). There was overlap among C16:0, C18:2, C18:3, and C20:2-OH but C18:0 and C18:1 were both significantly increased in the cultured embryos and C20:1-OH was 30% lower in the cultured embryos.

Rates of substrate uptake & carbon conversion efficiency: The culture medium and filter paper remaining in wells after embryos grew for 9 days (and in control wells without embryos) were recovered and analyzed by LC-MS/MS for media substrate (glucose, sucrose, and glutamine) concentration. The instrument peak values were normalized to the ^{13}C-internal standards (glucose and glycine), and then the corrected peak values of biological replicates (6

Table 2. Average rates of (A) accumulation (ug/embryo/day) of biomass components in unlabeled culture embryos vs. in planta embryos and (B) consumption (mM/day) of substrates in culturing medium by 18-27 DAP embryos. Standard deviations were generated from 3 (A) or 4 (B) biological replicates, and components that are significantly different are marked with an asterix.

(A)	Cultured Embryos		In Planta embryos		
	AVG	ST. DEV.	AVG	ST. DEV.	*p*-value
Fatty Acids	4.68	0.46	3.88	0.54	0.13
Proteins	5.80	0.26	5.05	0.55	0.13
Starch	0.66	0.17	0.50	0.24	0.19
*Cell Wall	6.89	0.60	4.72	1.00	0.04

(B)	uptake (mmol/day/embryo)	
	AVG	ST. DEV.
Glucose	125.8	1.1
Sucrose	13.3	1.3
Glutamine	18.3	1.4

Table 3. Carbon conversion efficiency determined by the carbon sink in biomass divided by the carbon uptake from media substrate

	mol C/emb
carbon uptake from glucose	6.77
carbon uptake from sucrose	1.44
carbon uptake from glutamine	0.81
total carbon uptake	9.02
	mol C/emb
carbon sunk in TAG	3.10
carbon sunk in protein	2.03
carbon sunk in starch	0.23
carbon sunk in cell wall	2.29
total carbon into biomass	7.66
Carbon Conversion Efficiency:	85.29%

without embryos, 8 with embryos) were averaged. The molar amount of media left in the wells was determined by multiplying the mass spectra peak area of media with embryos by the ratio of the peak area for media without embryos to the initial moles of substrate in the prepared medium. This amount remaining in wells was subtracted from the initial amount added to the wells, then divided by 9 for the rate per day and 10 for the rate per embryo, respectively (Table 2B). These values were converted to total moles of substrate carbon taken up by each embryo and divided by the carbon content of accumulated biomass per embryo to determine carbon conversion efficiency (Tables 2, 3). The carbon conversion efficiency is a measure of the extent to which the carbon taken up from the environment is converted into biomass components. For lesquerella, this efficiency was estimated to be 85%, which will be put in the context of other species in the discussion.

Tricarboxylic acid cycle labeling: Four cultures were performed under separate settings to examine labeling in lesquerella embryos. The first was an unlabeled control culture to verify the labeling analysis methods where the medium contained only unlabeled sucrose, glucose, and glutamine. The second culture that was performed contained 20% (w/w) labeled glucose, sucrose, and glutamine, with the rest of each unlabeled, to check the natural occurrence of ^{13}C isotopes in the embryos and to check the purity of the organic acid peaks analyzed by the LC-MS/MS. The third culture used labeled glucose, whose labeling was postulated to contribute the most to glycolysis and the oxidative pentose phosphate pathway. The fourth culture used labeled glutamine, whose labeling was hypothesized to affect amino acids and compounds of the TCA cycle, where it joins in at AKG.

The purification fraction containing organic acids produced results for citrate, isocitrate, AKG, succinate, fumarate, and malate. Oxaloacetate has been shown to be unstable in water and since metabolite extractions were performed in boiling water, this metabolite was not detected (Bajad et al., 2006). Since fumarate and AKG could lose a labeled carbon as carbon dioxide in the collision cell, daughter fragments mass spectra peaks, with or without that labeled carbon (m+[#carbon−1] and m+[#carbon]), had to be added up for the parent ions (see Supplementary 1). Each isotopomer value was converted to a percentage of that metabolite's total labeling within a sample. These relative values were corrected for the natural abundance of heavy isotopes in heteroatoms (H and O) that may affect analysis of carbon labeling. These corrected values are included in Supplementary 2.

Control results are mostly as expected, with M+0 mass isotopomer abundance (all unlabeled) all above 90% and a small abundance of M+1 (accounting for ^{13}C natural abundance)

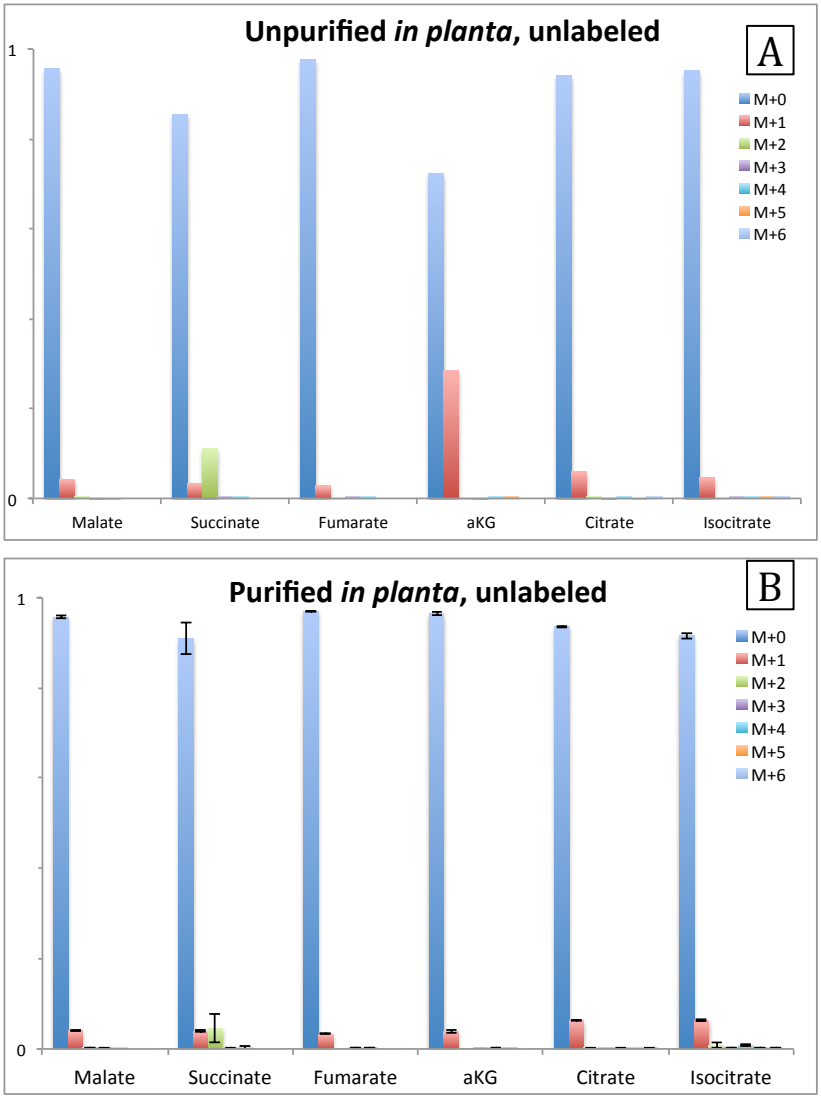

Figure 7. Purified and unpurified *in planta* labeling controls. (A) Unpurified *in planta* embryos show a high abundance of the M+1 isotopomer in AKG as well as a high abundance of the M+2 isotopomer in succinate. (B) Purified embryos display the expected abundance of M+1 in AKG and lower abundance of M+2 in succinate, but this value is still higher than expected.

making up the most part of the rest. Purification, shown in graphs of the unlabeled *in planta* samples, seems to have eliminated a contaminant that co-eluted with the M+1 isotopomer of AKG (Figure 7). However in data corresponding to both unpurified and purified samples, succinate showed unexpected results since it had a significantly higher abundance of the M+2 isotopomer than for M+1. This is inconsistent with the expectation that feeding embryos unlabeled substrates would result in unlabeled metabolite composition, with naturally occurring carbon isotopes being included at exponentially lower abundances for every additional carbon. Therefore analysis of organic acids should occur on purified OA fractions, but labeling of succinate cannot yet be definitively analyzed and will therefore be disregarded.

If isotopic steady state had been reached in the time of incubation it would be expected that in embryos cultured in 20% labeled substrates, 20% of the total carbon in intracellular

metabolites would be labeled. The average labeling per carbon in each metabolite is listed in Table 4. Despite a low average for fumarate, which is discussed below, these results indicate within reason that isotopic steady state was obtained in the 9-day incubation period of embryo growth under steady light.

Table 4. Averages and standard deviations of percent labeling per carbon in OAs of embryos grown with 20% labeled Suc, Glc and Gln (n=4).

Organic Acid	average labeling	st. dev.
Malate	21.2%	<0.1%
Succinate	20.9%	1.6%
Fumarate	16.4%	1.4%
aKG	20.0%	0.9%
Citrate	19.5%	0.1%
Isocitrate	19.9%	0.8%

In labeled glucose culture embryos, the In labeled glucose culture embryos, the ^{13}C is expected to be observed at the incorporation of acetyl-CoA, which is processed through glycolysis to end up with both carbons labeled (Figure 9). This is visible in experimental results using 20% [U-^{13}C6] glucose and 80% [1,2-^{13}C2] glucose as an increased abundance of the M+2 isotopomer in comparison to the M+1 isotopomer (Figure 8A). The inclusion of unlabeled glutamine is visible in the increase of the M+0 isotopomer at AKG. Results from the culture supplemented with 100% [U-^{13}C5] glutamine show its inclusion in the TCA cycle as the

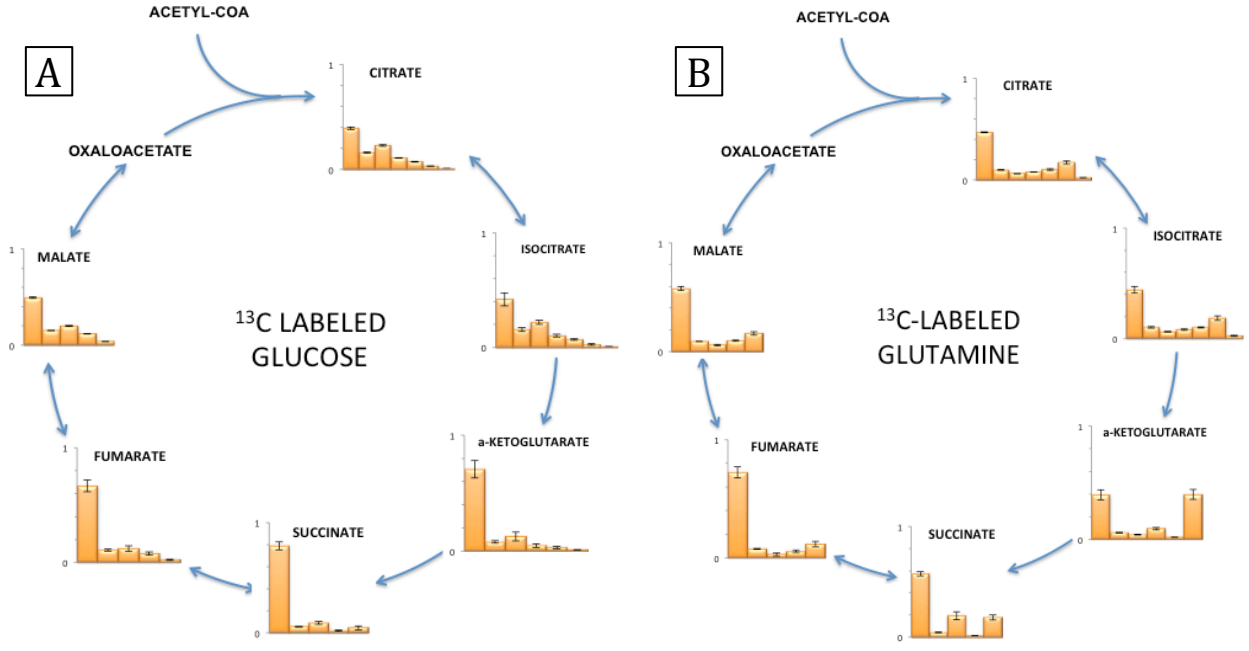

Figure 8. TCA cycle labeling. Mass isotopomer abundances of organic acids of the TCA cycle from (A) ^{13}C-labeled glucose cultured embryos and (B) ^{13}C-labeled glutamine cultured embryos.

abundant M+5 isotopomer, which is the most abundant isotopomer of AKG and the second most abundant of all the others (Figure 8B).

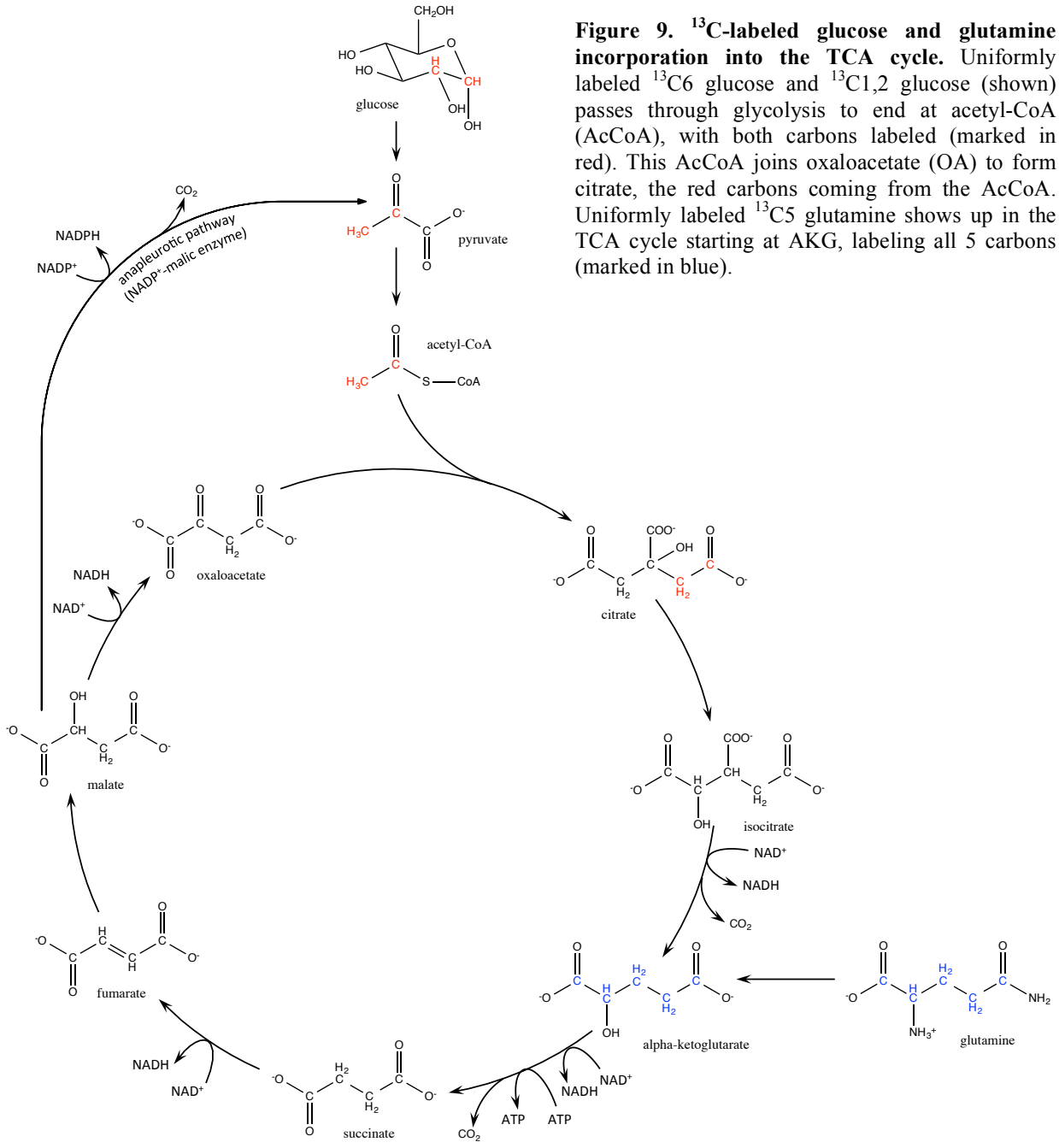

Figure 9. ^{13}C-labeled glucose and glutamine incorporation into the TCA cycle. Uniformly labeled ^{13}C6 glucose and ^{13}C1,2 glucose (shown) passes through glycolysis to end at acetyl-CoA (AcCoA), with both carbons labeled (marked in red). This AcCoA joins oxaloacetate (OA) to form citrate, the red carbons coming from the AcCoA. Uniformly labeled ^{13}C5 glutamine shows up in the TCA cycle starting at AKG, labeling all 5 carbons (marked in blue).

Discussion

This study aimed to validate conditions for obtaining ^{13}C-labeling data for building a flux map of lesquerella embryo metabolism. The culturing conditions determined that the average carbon conversion efficiency of lesquerella was 85%. This result contrasts greatly with the heterotrophic tissues of sunflower, which is estimated at 50% (Alonso et al., 2007) but is similar to developing *Brassica napus* embryos, estimated to be above 80% (Goffman et al., 2005). In *B. napus*, flux through the TCA cycle is nearly absent, reducing carbon loss as CO_2 (Goffman et al., 2005), and instead the light reactions of photosynthesis provide most of the ATP and reductant and RuBisCO bypasses the glycolytic reactions of the Calvin cycle, increasing the efficiency of glucose breakdown and oil synthesis (Schwender et al., 2004).

It is apparent from the significantly increased abundance of the M+2 isotopomers of TCA cycle organic acid intermediates in ^{13}C-labeled glucose lesquerella embryos that a portion of glycolysis goes into the cycle as acetyl-CoA. The significant increase in abundance of the M+0 isotopomer from isocitrate to AKG in the same culture, coupled with a high abundance of M+5 mass isotopomers in all organic acids from the ^{13}C-labeled glutamine culture indicates that the glutamine synthase, hydrolyzing glutamine to glutamate, and glutamate dehydrogenase, producing alpha-ketoglutarate by reducing $NAD(P)^+$, are both active in converting glutamine into AKG.

It was previously shown that maturing embryos direct the majority of their carbon intake towards fatty acid synthesis from 27 - 33DAP (Cocuron et al., 2014). NADPH, NADH, and ATP along with acetyl-CoA are essential for increased oil accumulation, and the activity of the glutamine converting pathway as well as the TCA cycle, both producing ATP and reductant, could be contributing to fatty acid synthesis. The fatty acid profile of cultured versus *in planta*

embryos showed discrepancies between C18:0, C18:1, and C20:1-OH. This might suggest that the pathway that leads from C18:1 to C20:1-OH is lagging in cultured embryos, which is currently being further investigated by examining cultures supplemented with herbicides. Used as inhibitors of fatty acid synthesis, these herbicide cultures might give insight into the metabolism of the yet-unknown lesquerolic acid biosynthetic pathway.

Succinate in both unpurified and purified *in planta* labeling analysis and also in labeled culture analysis showed an unexpected increase in abundance for M+2 mass isotopomer. It is possible that a contaminant not separated out in purification co-eluted with succinate, but further analysis is required to make any conclusions. Therefore, succinate labeling cannot be taken into account for flux modeling.

In the 20% control culture for determining isotopic steady state, fumarate was observed to reach about 16% labeling. A compound that does not reach 20% might indicate that there is a pool of unlabeled compound that is built up before the culture and stored in another compartment (e.g., the vacuole) and is not passing through the TCA cycle. This idea corroborates with previous data that shows only a very small increase in the total accumulation of embryonic fumarate between 18 and 27 DAP in comparison with the rest of the TCA organic acids which increase in much greater amounts (Cocuron et al., 2014) and is further supported by the labeling data in Figure 7B, where the M+0 of fumarate is in higher abundance that that of malate. In order to be used in carbon flux modeling, labeled fumarate abundance data must corrected for the diluting pool of unlabeled fumarate.

Similar analysis of organic acids for *Zea maize* embryos, including mass isotopomer distribution of the labeled metabolites and 20% labeling to confirm isotopic steady-state, has recently been published (Koubaa et al., 2013). These published results are different from the

ones achieved for lesquerella, despite very similar experimental methods. This highlights the necessity of performing these experiments for each plant species in order to build species-specific metabolic flux maps.

The key reason that only organic acids of the TCA cycle had been obtained up to this point was because of a problem with sugar labeling. The labeled glucose cultures included unlabeled sucrose, which gets stored in the vacuole and cleaved into unlabeled glucose and fructose by invertase. In extractions, vacuoles were lysed and these unlabeled sugars overwhelmed the labeled sugars accumulated during embryo growth and prevented accurate sugar labeling information.

Future Work

The labeling data obtained in this study in conjunction with future labeling data from sugars, phosphorylated compounds, and amino acids can be used to build a complete map of fluxes throughout embryo metabolism. To collect labeling data from all stable, water-soluble intracellular metabolites and then build a complete flux map of glycolysis, the oxidative pentose phosphate pathway, the TCA cycle, and the links between them, a way of bypassing the storage of unlabeled sugars in the vacuole needs to be found. The first option, now in progress, is to develop a culturing medium that does not include sucrose. The second option is to remove the vacuole by non-aqueous fractionation (Farré et al., 2001).

After obtaining all the necessary data, the *13CFLUX* software (obtained from Dr. W. Wiechert of the University of Siegen, Germany) will be used to mathematically model the data in the form of a metabolic flux map. The differences in mass isotopomer abundances between unequal neighboring compounds can be explained by linked metabolic pathways, and this

mathematical modeling software can be used to calculate the fluxes contributing to shared intracellular metabolites. Once the flux map has been built, and enzymatic targets limiting the production of ATP, reductant, or acetyl-CoA have been identified as engineering focuses, it will be necessary to identify and optimize a method for transformation. Both the *Agrobacterium tumefaciens*-mediated transformation of calli (Wang et al., 2008) and biolistic leaf plastid transformation (Skarzhinskaia et al., 2002) have shown to be possible methods.

Acknowledgements

For funding, acknowledgement goes to the The Ohio State University Start-Up Funds for Dr. Ana Paula Alonso.

I thank OSU's Targeted Metabolomics Laboratory (metabolomics.osu.edu) for access to the GC-MS and LC-MS/MS instruments, funded by the Center for Applied Plant Sciences (CAPS) and the Translational Plant Sciences Targeted Investment in Excellence (TIE), respectively.

Considerable appreciation goes to Dr. Venkat Gopalan and Dr. Enrico Bonello for their time and input as thesis committee members.

I also thank Gary Posey (greenhouse superintendent) for maintaining plant growth facilities.

Analyte	Mass isotopomer	Parent/daughter transition
Succinate	M+0	116.9/98/9
	M+1	117.9/99.9
	M+2	118.9/100.9
	M+3	119.9/101.9
	M+4	120.9/102.9
Malate	M+0	132.9/114.9
	M+1	133.9/115.9
	M+2	134.9/116.9
	M+3	135.9/117.9
	M+4	136.9/118.9
Fumarate	M+0	115.0/71.0
	M+1	116.0/71.0; 116.0/72.0
	M+2	117.0/72.0; 117.0/73.0
	M+3	118.0/73.0; 118.0/74.0
	M+4	119.0/74.0
AKG	M+0	145.0/101.0
	M+1	146.0/101.0; 146.0/102.0
	M+2	147.0/102.0; 147.0/103.0
	M+3	148.0/103.0; 148.0/104.0
	M+4	149.0/104.0; 149.0/105.0
	M+5	150.0/105.0
Citrate	M+0	191.0/173.0
	M+1	192.0/174.0
	M+2	193.0/175.0
	M+3	194.0/176.0
	M+4	195.0/177.0
	M+5	196.0/178.0
	M+6	197.0/179.0
Isocitrate	M+0	191.0/173.0
	M+1	192.0/174.0
	M+2	193.0/175.0
	M+3	194.0/176.0
	M+4	195.0/177.0
	M+5	196.0/178.0
	M+6	197.0/179.0

Supplementary 1. Parent/Daughter isotopomer pairs optimized for LC-MS/MS analysis

		Purified						Unpurified			
		In Planta		13C-Glucose labeled		13C-Glutamine labeled		In Planta	20% labeled		
analyte	Mass isotopomer	average % abundance	st. dev. % abundance	average % abundance	st. dev. % abundance	average % abundance	st. dev. % abundance	average % abundance	average % abundance	st. dev. % abundance
Malate	M+0	0.957	0.002	0.493	0.008	0.580	0.019	0.956	0.489	0.010
	M+1	0.041	0.001	0.152	0.004	0.094	0.001	0.043	0.153	0.004
	M+2	0.002	0.001	0.199	0.005	0.060	0.007	0.001	0.201	0.006
	M+3	0.000	0.000	0.119	0.003	0.101	0.006	0.000	0.120	0.002
	M+4	0.000	0.000	0.038	0.001	0.168	0.016	0.000	0.038	0.001
Succinate	M+0	0.910	0.035	0.790	0.037	0.572	0.019	0.855	0.697	0.033
	M+1	0.040	0.003	0.056	0.003	0.043	0.004	0.032	0.066	0.003
	M+2	0.046	0.031	0.090	0.014	0.195	0.037	0.110	0.140	0.017
	M+3	0.001	0.002	0.020	0.005	0.013	0.001	0.003	0.030	0.006
	M+4	0.003	0.005	0.045	0.018	0.178	0.022	0.000	0.068	0.012
Fumarate	M+0	0.970	0.000	0.668	0.051	0.725	0.047	0.976	0.621	0.027
	M+1	0.033	0.000	0.109	0.010	0.075	0.004	0.028	0.126	0.008
	M+2	-0.006	0.000	0.121	0.025	0.029	0.014	0.000	0.140	0.016
	M+3	0.002	0.001	0.079	0.015	0.055	0.009	0.002	0.085	0.007
	M+4	0.002	0.001	0.025	0.005	0.118	0.023	0.000	0.028	0.003
aKG	M+0	0.964	0.003	0.707	0.075	0.392	0.044	0.723	0.638	0.017
	M+1	0.040	0.004	0.079	0.010	0.060	0.005	0.284	0.088	0.006
	M+2	-0.006	0.001	0.127	0.039	0.041	0.004	0.000	0.170	0.009
	M+3	0.000	0.000	0.046	0.015	0.095	0.012	0.000	0.054	0.003
	M+4	0.002	0.000	0.031	0.011	0.020	0.003	0.001	0.038	0.002
	M+5	0.000	0.000	0.011	0.003	0.397	0.044	0.000	0.013	0.001
Citrate	M+0	0.935	0.001	0.392	0.012	0.469	0.005	0.941	0.377	0.006
	M+1	0.063	0.000	0.159	0.006	0.099	0.003	0.059	0.162	0.005
	M+2	0.000	0.001	0.229	0.009	0.061	0.003	0.000	0.236	0.006
	M+3	0.000	0.000	0.108	0.003	0.078	0.001	0.000	0.111	0.003
	M+4	0.001	0.000	0.073	0.004	0.102	0.008	0.000	0.075	0.002
	M+5	0.000	0.000	0.031	0.002	0.172	0.017	0.000	0.032	0.001
	M+6	0.001	0.000	0.008	0.001	0.022	0.001	0.000	0.008	0.001
Isocitrate	M+0	0.915	0.006	0.419	0.056	0.442	0.030	0.952	0.377	0.019
	M+1	0.063	0.002	0.157	0.018	0.102	0.006	0.046	0.165	0.004
	M+2	0.008	0.007	0.219	0.019	0.063	0.003	0.000	0.233	0.009
	M+3	0.002	0.001	0.103	0.012	0.082	0.006	0.000	0.117	0.009
	M+4	0.008	0.002	0.070	0.008	0.102	0.004	0.002	0.073	0.006
	M+5	0.002	0.000	0.026	0.008	0.186	0.021	0.002	0.030	0.001
	M+6	0.002	0.002	0.007	0.004	0.026	0.004	0.005	0.005	0.001

Supplementary 1. Corrected isotopomer abundance averages for labeled and unlabeled cultures.

References

Abbott Thomas P, Y. Victor Wu, Kenneth D. Carlson, Morey E. Slodki, and Robert Kleiman (1994). Isolation and Preliminary Characteristization of *Lesquerella fendleri* Gums from Seed, Presscake, and Defatted Meal. *J. Agric. Food Chem.,* 42: 1678-1685.

Bajad Sunil U., Wenyun Lu, Elizabeth H. Kimball, Jie Yuan, Celeste Peterson, and Joshua D. Rabinowitz (2006). Separation and quantitation of water soluble cellular metabolites by hydrophilic interaction chromatography-tandem mass spectrometry. *J. Chromatogr. A*, 1125: 76-88.

Barclay Arthur S., Howard S. Gentry, and Quentin Jones (1962). The Search for New Industrial Crops II: Lesquerella (Cruciferae) as a Source of New Oilseeds. *Econ. Bot.*, 16(2): 95-100.

Brahim Kebe, David K. Stumpf, Dennis T. Ray, and David A. Dierig (1996). *Lesquerella fendleri* seed oil content and composition: Harvest date and plant population effects. *Ind. Crops Prod.*, 5: 245-252.

Broun Pierre and Chris Somerville (1997). Accumulation of Ricinoleic, Lesquerolic, and Densipolic Acids in Seeds of Transgenic Arabidopsis Plants That Express a Fatty Acyl Hydroxylase cDNA from Castor Bean. *Plant Physiol.,* 113: 933-942.

Carlson Kenneth D., A. Chaudhry, and Marvin O. Bagby (1990). Analysis of Oil and Meal from *Lesquerella fendleri* Seed. *J. Am. Oil Chem. Soc.*, 67(7): 438-442.

Cermak Steven C., Kendra B. Brandon, and Terry A. Isbell (2006). Synthesis and physical properties of estolides from lesquerella and castor fatty acid esters. *Ind.Crops Prod.*, 23: 54-64.

Cocuron Jean-Christophe, Brooke Anderson, Alison Boyd, Ana Paula Alonso (2014). Targeted metabolomics of *Physaria fendleri*, an industrial crop producing hydroxy fatty acids. *Plant Cell Phys.*, 55(3): 620-633.

Dierig David A., Guangyao Wang, William B. McCloskey, Kelly R. Thorp, Terry A. Isbell, Dennis T. Ray, and Michael A. Foster (2011). *Lesquerella*: New crop development and commercialization in the U.S. *Ind. Crops Prod.*, 34: 1381-1385.

Farré Eva M., Axel Tiessen, Ute Roessner, Peter Geigenberger, Richard N. Trethewey, and Lothar Willmitzer (2001). Analysis of the Compartmentation of Glycolytic Intermediates, Nucleotides, Sugars, Organic Acids, Amino Acids, and Sugar Alcohols in Potato Tubers Using a Nonaqueous Fractionation Method. *Plant Phys.*, 127(2): 685-700.

Goffman Fernando D., Ana P. Alonso, Jorg Schwender, Yair Schachar-Hill, John B. Ohlrogge (2005). Light enables a very high efficiency of carbon storage in developing embryos of rapeseed. *Plant Phys.*, 138: 2269-2279.

Goodrum John W. and Daniel P. Geller (2004). Influence of fatty acid methyl esters from hydroxylated vegetable oils on diesel fuel lubricity. *Bioresour. Technol.*, 96: 851-855.

Kim Kyoung-Rok and Deok-Kun Oh (2013). Production of hydroxy fatty acids by microbial fatty acid-hydroxylation enzymes. *Biotechnol. Adv.*, 31: 1473-1485.

Koubaa Mohamed, Jean-Christophe Cocuron, Brigitte Thomasset, and Ana Paula Alonso (2013). Highlighting the tricarboxylic acid cycle: Liquid and gas chromatography-mass spectrometry analyses of ^{13}C–labeled organic acids. *Anal. Biochem.*, 436(2): 151-159.

Moon Hangsik, Mark A. Smith, and Ljerka Kunst (2001). A Condensing Enzyme from the Seeds of *Lesquerella fendleri* that Specifically Elongates Hydroxy Fatty Acids. *Plant Physiol.*, 127(4): 1635-1643.

Mutlu Hatice and Michael A.R. Meier (2010). Castor oil as a renewable resource for the chemical industry. *Eur. J. Lipid Sci. Technol.*, 112: 10-30.

Skarzhinskaya Marina, Maria Landgren, and Kristina Glimelius (1996). Production of intertribal somatic hybrids between *Brassica napus* L. and *Lesquerella fendleri* (Gray) wats. *Theor. Appl. Genet.*, 93(8): 1242-1250.

Schwender Jorg, Fernando Goffman, John B. Ohlrogge, Yair Shachar-Hill (2004). Rubisco without the Calvin cycle improves the carbon efficiency of developing green seeds. *Nature*, 432: 779-782.

Thompson Anson E. and David A. Dierig (1994). Initial selection and breeding of *Lesquerella fendleri*, a new industrial oilseed. *Ind. Crops Prod.*, 2(2): 97-106.

Wu Y. Victor and Thomas P. Abbott (1996). Enrichment of gum content from *Lesquerella fendleri* seed coat by air classification. *Ind. Crops Prod.*, 5: 47-51.